ORIGINAL PAPER

Genetic analysis of *opaque2* modifier loci in quality protein maize

**David R. Holding · Brenda G. Hunter · Taijoon Chung · Bryan C. Gibbon ·
Clark F. Ford · Arvind K. Bharti · Joachim Messing · Bruce R. Hamaker ·
Brian A. Larkins**

Abstract Quality protein maize (QPM) was created by
selecting genetic modifiers that convert the starchy endo-
sperm of an *opaque2* (*o2*) mutant to a hard, vitreous pheno-
type. Genetic analysis has shown that there are multiple,
unlinked *o2* modifiers (*Opm*), but their identity and mode
of action are unknown. Using two independently developed
QPM lines, we mapped several major *Opm* QTLs to chro-
mosomes 1, 7 and 9. A microarray hybridization performed
with RNA obtained from true breeding *o2* progeny with vit-
reous and opaque kernel phenotypes identified a small
group of differentially expressed genes, some of which map
at or near the *Opm* QTLs. Several of the genes are associated
with ethylene and ABA signaling and suggest a potential
linkage of *o2* endosperm modification with programmed
cell death.

Introduction

Cereals typically provide 50% of the dietary protein for
humans and can comprise 70% of the protein intake for
people in developing countries (Deutscher 1978). The
demand for cereal grains, especially maize (Pingali 2001),
will continue to increase as a consequence of the expanding

D. R. Holding · B. G. Hunter · T. Chung ·
B. C. Gibbon · B. A. Larkins (✉)
Department of Plant Sciences, University of Arizona,
Forbes Hall 303C, Tucson, AZ 85721, USA
e-mail: larkins@ag.arizona.edu

Present Address:
T. Chung
Department of Genetics, University of Wisconsin-Madison,
425-G Henry Mall, Madison, WI 53706-1580, USA
e-mail: tchung2@wisc.edu

B. C. Gibbon
Department of Biology, Baylor University,
One Bear Place, Waco, TX 76798, USA
e-mail: bryan_gibbon@baylor.edu

C. F. Ford
Department of Food Science and Human Nutrition,
Iowa State University, 2312 Food Sciences Bldg.,
Ames, IA 50011, USA
e-mail: cfford@iastate.edu

A. K. Bharti · J. Messing
Waksman Institute of Microbiology,
Rutgers University, Piscataway, NJ 08854-8020, USA
e-mail: bharti@waksman.rutgers.edu

J. Messing
e-mail: messing@waksman.rutgers.edu

B. R. Hamaker
Department of Food Science, Purdue University,
West Lafayette, IN 47907, USA
e-mail: hamakerb@purdue.edu

human population, which could increase by another billion people by the year 2020 (Vasil 1998). However, it is well known that cereals do not provide a nutritionally balanced source of protein. The most abundant proteins they contain, the prolamin storage proteins, are devoid of several amino acids essential for monogastric animals, with lysine most limiting (Bhan et al. 2003). Most cereal grains contain 1.5–2% lysine, while 5% is required for optimal human nutrition (Young et al. 1998).

Discovery that the *opaque2* (*o2*) mutation increases the lysine content in maize endosperm by decreasing the synthesis of prolamin (zein) proteins and increasing the level of other types of endosperm proteins raised expectations for the genetic improvement of cereal protein quality (Munck 1992). However, the low seed density and soft kernel texture of this type of mutant were associated with a number of inferior agronomic traits, including brittleness and insect susceptibility. With only a few exceptions (Habben and Larkins 1995), these mutants were not commercially developed. Shortly after the discovery of *o2*, maize breeders became aware of the existence of genes that alter the soft, starchy texture of *o2* endosperm, giving it a normal appearance. The loci controlling this trait, designated "*o2* modifiers" (*Opm*), proved to be genetically complex but nevertheless effective in ameliorating the negative features of the opaque kernel phenotype (Vasal et al. 1980; Geevers and Lake 1992). By systematically introgressing *Opm* genes into *o2* germplasm, plant breeders at the International Maize and Wheat Improvement Center in Mexico (CIMMYT) (Vasal et al. 1980) and Pietermarizburg, South Africa (Geevers and Lake 1992) were able to develop several modified *o2* mutants that they designated "Quality Protein Maize", or QPM. QPM has the phenotype and yield of normal maize, but the high lysine content of *o2* (Mertz 1992; Prasanna et al. 2001).

The development and widespread use of QPM germplasm have been implemented slowly. In part, this is because of the technical complexity of introducing multiple *Opm* loci, while maintaining a homozygous *o2* locus and monitoring the amino acid composition (Vasal et al. 1980). This process could be greatly accelerated if the identities of *Opm* genes were known, but unfortunately relatively little is known about their number, chromosomal location, and mechanism of action. Indeed, the factors responsible for the formation of vitreous and starchy endosperm in maize are poorly understood (Séne et al. 2001; Holding and Larkins 2006). Using a limited set of RFLP markers and bulked segregant analysis (BSA) (Michelmore et al. 1991), Lopes et al. (1995) identified two chromosomal regions on the long arm of chromosome 7 that are associated with *o2* endosperm modification. The locus near the centromere is linked with the gene encoding the 27-kDa γ-zein, while the other locus, identified by a single RFLP, is at the distal end

of chromosome 7, near the telomere. Evaluation of kernel density and content of 27-kDa γ-zein in a set of recombinant inbred lines (RILs) developed from a Pool 33 QPM by W64A*o2* cross revealed tight linkage of the 27-kDa γ-zein locus in Pool 33 QPM with the vitreous phenotype, but it was not possible to determine the role of this protein in the formation of the vitreous phenotype.

To increase our knowledge of the number and relationships between *Opm* loci, we analyzed two different QPMs, one from South Africa, K0326Y (Geevers and Lake 1992), and CM105*Mo2*, which we derived from a cross between CM105*o2* and CIMMYT's Pool 33 QPM (Gibbon et al. 2003). Crosses were made to W64A*o2*, a soft, starchy Midwestern inbred line, and F2 and F3 populations were created for phenotypic and genotypic analysis. Initially, the BSA approach was used to identify QTLs, because it was difficult to accurately phenotype kernels with intermediate degrees of vitreousness. We subsequently developed a method using a digital camera to quantitatively measure kernel vitreousness (defined by the extent to which kernels transmit light), and we applied this procedure in conjunction with measurements of density and hardness to identify QTLs affecting these traits. Results of the BSA showed that K0326Y QPM and CM105*Mo2* (Pool 33 QPM) share a common QTL near the centromere of chromosome 7 that appears to have a major effect on *o2* endosperm modification. Additional loci associated with vitreousness were found on chromosome 9 (K0326Y QPM) and chromosome 6 (CM105*Mo2*). Analysis of individual kernels from another F2 population developed from the K0326Y QPM by W64A*o2* cross confirmed the presence of QTLs on chromosomes 7 and 9. In addition, five other QTLs were found, one each on chromosomes 5S, 7L and 10S, and two on chromosome 1L. These results indicated that the QTL near the centromere of chromosome 7 has a major effect on endosperm texture (30% of the variance), while the other six QTLs have smaller effects (5–12% of the variance). Microarray and real-time PCR comparisons of RNA transcripts from vitreous and soft kernels of the K0326Y QPM by W64A*o2* cross identified several candidate genes that were up-regulated in modified *o2* and coincide with QTLs identified in bins 1.05, 7.02, and 9.05.

Materials and methods

Plant materials

Maize genetic materials were grown at the University of Arizona West Campus Agricultural Center, Tucson, Arizona, between 2001 and 2006. K0326Y QPM, a modified *o2* inbred line developed in South Africa (Geevers and Lake 1992), was provided by H. Geevers. CM105*Mo2* is a

QPM inbred line developed at the University of Arizona by introgression of the *o2* modifier genes from Pool 33 QPM into CM105*o2* (Gibbon et al. 2003). Pool 33 QPM, which was provided by CIMMYT, was described by Vasal et al. (1980) and Bjarnason and Vasal (1992). W64A*o2* is an opaque (starchy endosperm) Midwestern dent inbred line originally obtained from Purdue University, West Lafayette, Indiana. Bulk segregant analysis (BSA) (Michelmore et al. 1991) was done using F2 populations obtained by controlled pollination of F1 plants from reciprocal crosses of either K0326Y QPM by W64A*o2* or CM105*Mo2* by W64A*o2*. The F2 kernels were examined with a light box and classified as vitreous or opaque, according to the degree of light transmission through the endosperm. Vitreous and opaque F2 kernels were planted, and ears from these (F3) plants were self pollinated to verify true-breeding uniformity for kernel phenotypes. For the K0326Y QPM by W64A*o2* cross, vitreous and opaque bulks composed of 40 individuals each were made, and for the CM105*Mo2* by W64A*o2* cross each bulk contained 29 individuals. Leaf tissues from the parental inbreds, F1 plants and F2 individuals were collected, lyophilized and stored for subsequent analysis.

A second mapping population of the K0326Y QPM × W64A*o2* cross was created from a well-filled F2 ear. Three hundred kernels were removed from the middle of the ear and measured for vitreousness using a digital camera (see below). The seeds were germinated and DNA was recovered from 229 seedlings.

Single kernel measurements of vitreousness

Individual kernels were mounted in small holes cut in cardboard, and placed on a light box. Light transmission was recorded with a digital camera and measured in arbitrary units using Adobe Photoshop (Adobe, San Jose, CA).

Kernel hardness

Kernel hardness was evaluated by two methods: a grinding test using a micro-hammer mill (Glen Mills Inc., Clifton, NJ) (Li et al. 1996) and a compression method using a MTS Sintech 10 Universal Testing Machine (Eden Prairie, MN, 1,000 lb load cell). Kernels were conditioned at 27°C and 67% relative humidity before evaluation. For the grinding test, 20 g kernel samples were passed through the mill at 3,600 rpm and time (s) was recorded for tube fill to 17 mL volume. In the compression test, kernels were placed germ side up on a plate and deformed until breakage using a MTS *Q* Test Universal Testing Machine (Eden Prairie, MN, 1,000 lb load cell). Peak load (kg) and energy to peak load (kg/mm) were recorded.

Analysis of seed density

The density of kernels, defined as the ratio of kernel weight to measured volume, was determined for the parents, F1 and F3 individuals that composed the vitreous and opaque bulks using a pycnometer (Stereopycnometer Quantachrome Corp., Syosset, NY) or by volume displacement. The measurement is based on Archimede's principle of fluid or gas displacement to determine the volume. Samples were weighed in a sample cell holder of known volume. The cell was then placed in the pycnometer and pressurized with nitrogen gas to approximately 17 psig. After the reading stabilized, it was recorded. The sample volume was determined and density calculated. Alternatively, kernels were placed in a 500 mL cylinder and the weight recorded. The cylinder was then filled with absolute ethanol (200 proof, density 0.78612 at room temperature) and the volume and weight recorded. Seed density was calculated following the methods of Kniep and Mason (1989).

Preparation of DNA

DNA for the BSA was extracted from lyophilized leaf tissue of individuals that bred true for the vitreous or opaque kernel phenotypes. Young leaves from each F2 plant were ground in liquid nitrogen in the presence of acid washed sand, and the DNA was prepared by the CTAB method (Shen et al. 1994). To increase the purity of the DNA, samples were diluted in 500 μL TE buffer (10 mM Tris–HCl and 1 mM EDTA, pH 8.0) containing DNAse-free pancreatic RNAse (20 μg/mL) and incubated at 37°C for 30 min. This solution was extracted with an equivalent volume of phenol–chloroform saturated with Tris–HCl, pH 8.0, and then with chloroform alone. After precipitation with 2.5 volumes of ethanol and 0.1 volume of 3 M sodium acetate, pH 5.3, and washing with 70% ethanol, the DNA was dissolved in sterile water and the concentration determined with a NanoDrop Spectrophotmeter ND-100 (NanoDrop Technologies, Wilmington, DE). An equal amount of DNA from each F2 individual was combined to generate the bulked sample for SSR marker analysis.

For the K0326Y QPM × W64A*o2* F2 mapping population, DNA was extracted from ~3 cm^2 of fresh leaf tissue excised from 14-day-old seedlings. The tissue was placed in a 1.5 mL microcentrifuge tube and ground for 30 s at room temperature in 600 μL of urea buffer (7 M urea, 0.3125 M sodium chloride, 50 mM Tris–HCl, 20 mM EDTA, 1% sarkosyl, pH 8.0). 500 μL of phenol/chloroform/isoamyl alcohol (25:24:1) was added and the tubes were shaken at room temperature for 5 min. The samples were centrifuged for 5 min at 12,000g in a microcentrifuge, the aqueous phase transferred to a new tube, and 50 μL of 3 M sodium acetate, pH 5, and 500 μL of cold isopropanol

were added to precipitate the DNA. The tubes were incubated at room temperature for 10 min, and the DNA was recovered by centrifugation for three minutes at 12,000*g*. The DNA pellet was washed with 70% ethanol, air dried for 10 min, and resuspended in 50 μL of sterile water. For PCR reactions, the DNA samples were diluted to a final concentration of ∼20 ng/μL.

PCR analysis

The selection of DNA primers (Invitrogen, Carlsbad, CA) was based on mapped SSRs described in the Maize Genome Database (Lawrence et al. 2007; http://www.maizegdb.org). An effort was made to have at least one informative SSR per bin in order to effectively cover the entire maize genome. PCR reactions were performed using Taq DNA polymerase (New England BioLabs, Ipswich, MA) and buffer, with the addition of 1 M betaine and 2% DMSO, in a Peltier Thermal Cycler PTC-200 (MJ Research, Waltham MA) or an Eppendorf MasterCycler (Eppendorf, Westbury, NY). The PCR parameters were as follows: initial melting at 94°C for 2 min, then seven cycles of touch-down PCR with the annealing temperature declining from 62 to 56°C (94°C for 45 s, annealing for 45 s, 72°C for 45 s) followed by 35 cycles (94°C for 45 s, 55°C for 45 s, 72°C for 45 s) and a final extension cycle at 72°C for 5 min. The PCR products were separated by electrophoresis in 4% SFR agarose (Amresco, Solon, OH) and visualized by staining with ethidium bromide.

Linkage analysis and QTL detection

A linkage map for the F2 population from the cross between K0326Y QPM and W64A*o2* was determined using 140 informative SSR markers (Lawrence et al. 2007; http://www.maizegdb.org) with Map Manager QTX (Manly et al. 2001). In a few instances there were small discrepancies with regard to the marker order specified in Maize GDB as compared with the Map Manager QTX-generated map, but the SSR marker order determined by Map Manager QTX was used in this analysis. One thousand permutation tests were carried out to establish the significant threshold values, and simple QTL analysis was performed.

DNA sequencing and BAC assembly

The BAC clone ZMMBBb0049I19 belongs to the genomic library of *Zea mays* ssp. *mays* inbred B73, which was constructed by partial digestion with *Hin*dIII (Tomkins et al. 2002, Yim et al. 2002). This clone was anchored to the fingerprinted contig (FPC) #314 of the maize physical map on chromosome 7 using various markers (CL2764, CL1979, PCO123780, PCO137477 and zp27). The size of

the clone was estimated to be 151,600 bp based on the agarose FPC fingerprinted map.

BAC DNA was isolated using the Large Construct Kit (Qiagen) and then hydro-sheared into random fragments of two different sizes. Both size inserts were cloned into pUC119. Shotgun library #1 consisted of fragments ranging from 2.5 to 4 kb, while library #2 contained inserts of 5–7 kb. Nine plates of library #1 and 6 plates from library #2 were sequenced from both ends with universal primers (Vieira and Messing 1982) using the BigDye Terminator Cycle Sequencing Ready Reaction kit (Applied BioSystems) on an automated capillary sequencer (ABI 3730xl). In addition to shotgun sequencing, the BAC was also sequenced from both ends using T7 and SP6 primers in order to aid in the assembly process.

BAC assembly was carried out using PhredPhrap (Ewing et al. 1998; Ewing and Green 1998) and viewed using Consed (Gordon et al. 1998). The final assembly is in four un-ordered pieces (Phase 1) with two physical gaps, because of which the orientation of the middle two pieces cannot be confirmed. However, the order of the middle two pieces is confirmed due to presence of multiple bridge clones. The orientation of the first and fourth piece could also be confirmed by anchoring the BAC end sequences at their ends. The assembly size of the BAC clone ZMMBBb0049I19 is 163,263 bp.

Microarray analysis

Seeds of F3 individuals from the K0326Y QPM × W64A*o2* cross that were true-breeding for vitreous and opaque phenotypes were planted, and 18 DAP self-pollinated ears (with developing F4 seed) frozen in liquid nitrogen. Totally, 20 ears of each phenotypic class were used to create four pools of 25 vitreous kernels (V1–V4) and four pools of opaque kernels (O1–O4). Each pool consisted of five randomly chosen kernels from each of five of the 20 ears (25 kernels total per pool). Kernels were defrosted slightly, the pericarp and germ were removed and the endosperm was immediately refrozen. Total RNA was isolated according to the protocol described by Holding et al. (2007) and subsequently treated with DNAse1 (Roche, Pleasanton, CA) and re-purified with RNeasy cleanup columns (Qiagen, Valencia, CA), both according to the manufacturer's instructions. The experiment employed four microarrays and four biological replicates for each phenotype and incorporated a dye swap as follows: Array 1: V1 cy5, O1 cy3; Array 2: V2 cy5, O2 cy3; Array 3: V3 cy3, O3 cy5; Array 4: V4 cy3, O4 cy5.

One microgram RNA samples were used to make Cy3- and Cy5-labeled targets with a three step protocol as follows: (1) cDNA was synthesized using an oligo-(d)T primer that incorporated the T7 promoter; (2) targets were

amplified using in vitro transcription to produce aminoal-lyl-labeled cRNA; and (3) aminoallyl-labeled cRNA was coupled to Cy-labeled dyes. Details of these protocols can be found at: http://www.maizearray.org/files/cRNA_Target_Production_Using_RNA_Amplification.pdf.

Targets were hybridized to the maize 46 K (version 1) 70-mer oligo array printed on a single slide (details of which can be found at http://www.maizearray.org; the hybridization protocol can be found at http://www.maizearray.org/files/Hybridization_Protocol_For_cRNA_Targets.pdf).

Slides were scanned using a GenePix Autoloader 4200AL microarray scanner (Molecular Devices). Intensity values were normalized using the VSN (variance stabilized normalization) function of the "R" for Windows package. Despite the fact that the array hybridizations were very clean with no detectable background, all spots generate an intensity value expressed in natural log form. Consequently, the gene filter function of R was applied to the normalized values. The filter was set to give a "true" flag to array probes in which at least four of the eight pools gave expression values of 3.9 or more (49 absolute expression units). Probes were flagged as "false" if more than four pools gave expression values of below 3.9. Using these criteria, 28,736 probes were defined as true, and 17,392 were defined as false (of 46,128). The flagged expression values were imported into Excel and the false probes were excluded from further analysis. The Statistical Analysis for Microarrays (SAM) package of Microsoft Excel was used to identify differentially expressed probes (candidate *o2* modifiers). The raw and normalized microarray data sets are available at NCBIGEO (Accession # GSE10449, platform # GPL6438).

Mapping and expression verification of candidate *o2* modifiers

Oligonucleotide sequences corresponding to genes differentially expressed in vitreous and opaque endosperms were retrieved from the maize array website and used in BLASTN searches against all maize sequences in GenBank. Perfect matches to EST contigs submitted to Genbank by the Maize Mapping Project were selected. By using these contigs to search the MaizeGDB mapping database (http://www.maizegdb.org/), map positions were established for the majority of the differentially expressed genes. All map positions were taken from the May 2007 composite IBM/FPC map build. For sequences that did not match a mapped EST contig, the BLASTN reports were analyzed to look for perfect matches to maize BAC sequences. For these genes the physical map position was consulted in the maize FPC map at the Arizona Genomics Institute (http://www.genome.arizona.edu/fpc/maize/). A genomic contig containing the BAC was analyzed for nearby genetic markers that could be anchored to the genetic map at MaizeGDB.

Real time PCR was used to verify the results obtained in the microarray experiment. Primers were designed to amplify a 100–200 bp region of the EST contig sequence using the primer 3 software available at http://frodo.wi.mit.edu/. All primers were designed for a 60°C annealing temperature, and their sequences are shown in Supplemental Table 2. One microgram of samples of the DNAse 1-treated total RNA pools used for the microarray hybridization (V1–V4 and O1–O4) were used as templates for cDNA synthesis in 50 μL volumes using Superscript 2 (Invitrogen, Carlsbad, CA), according to the manufacturer's instructions. cDNAs were diluted 10-fold in water and amplified using the LightCycler fast start DNA master plus sybr green 1 kit (Roche, Pleasanton, CA) according to the manufacturer's instructions. The LightCycler 1.5 carousel thermocycler was used with the following program: 95°C for 5 min, followed by 45 cycles of 95°C for 10 s, 60°C for 5 s and 72°C for 10 s with 20°C per s ramp rates. Melting curves were obtained by heating from 65 to 95°C with a 0.1°C per s ramp rate. Relative expression levels of candidate genes in the vitreous and opaque pools were calculated using actin expression as a control, since it was repeatedly shown in preliminary experiments not to be differentially expressed between the vitreous and opaque samples. For each gene tested, the average crossing point (Cp) value for the four vitreous and opaque pools was made, and the relative expression calculated using the following equation where X = gene of interest, A = actin, V = V1 to V4 average Cp, O = O1 to O4 average Cp: $2^{[(VX - VA) - (OX - OA)]}$. The reciprocal of the resulting value is the fold-increase in the vitreous samples. Negative values indicate a decrease in the vitreous relative to the opaque kernels. The final fold-change values are the mean of the fold-change values from three independent experiments (±standard deviation).

Results

Identification of *Opm* QTLs based on BSA

QPM was developed independently by plant breeders in South Africa (Geevers and Lake 1992) and at CIMMYT (Vasal et al. 1980), and the number and relationship between the *Opm* loci in these genetic backgrounds is unknown. To investigate this question, we crossed K0326Y QPM and CM105*Mo2* with W64A*o2*. F2 individuals that were true-breeding for vitreous and opaque kernel phenotypes were identified by selfing, and DNA from leaf tissue was pooled to create samples for the BSA. Theoretically, the bulked DNA samples should contain common genomic regions associated with modified *o2* endosperm modifica-

Table 1 Phenotypic characterization of K0326Y QPM and W64Ao2 inbred lines, reciprocal F1s, and pooled vitreous and opaque F3 progeny from the K0326Y × W64Ao2 cross

Phenotype	K0326Y QPM (P1)	W64Ao2 (P2)	F1P1 × P2	F1P2 × P1	Vitreous bulk	Opaque bulk
Vitreousness	187.6 ± 20.9 a	31.1 ± 12.6 bc	169.1 ± 30.5 a	55.3 ± 18.9 b	169.0 ± 74.6 a	17.4 ± 6.0 bc
Density (g/mL)	1.3 ± 0.03 a	1.1 ± 0.02 b	1.3 ± 0.05 a	1.2 ± 0.02 ab	1.3 ± 0.1 a	1.1 ± 0.08 b
Grinding test (s)	14.3 ± 0.6 a	9.0 ± 0.0 b	15.6 ± 0.6 a	11.0 ± 1.7 b	13.3 ± 0.6 a	6.0 ± 0.0 c
Peak load (kg)	75.3 ± 40.2 a	16.4 ± 8.3 b	65.9 ± 35.4 a	45.8 ± 38.2 a	62.7 ± 46.5 a	20.5 ± 11.4 b
Energy to peak load (kg/mm)	22.5 ± 19.2 a	3.9 ± 3.1 b	52.6 ± 41.5 c	22.3 ± 32.6 a	32.4 ± 41.8 a	11.1 ± 10.3 b

Each value is the average and standard deviation for the endosperm traits analyzed as described in "Materials and methods". Within a row, values with the same letter are not significantly different at $P = 0.05$, based on the least significance difference (LSD) method

tion and a randomized background of unlinked genetic loci (Michelmore et al. 1991).

The phenotypic characteristics of the parents and progeny of the K0326Y QPM by W64Ao2 cross are shown in Table 1. Vitreousness was measured with a digital camera, and hardness was measured with both the Stenvert and the Instron assays. The results showed that kernels from the K0326Y QPM parent are more vitreous, denser and harder than the W64Ao2 parent, and that these phenotypes were observed in pooled samples made from F3 vitreous and opaque progeny. An *Opm* gene dosage effect was observed in the reciprocal F1 crosses, which showed intermediate degrees of vitreousness, hardness and density. This is a consequence of the triploid nature of the endosperm, which creates complex dosage effects, especially when multiple loci are involved (Lopes and Larkins 1995). For the CM105*Mo2* by W64A*o2* cross, only data for vitreousness and density were collected (Table 2). Here again kernels from ears homozygous for the *Opm* alleles were more vitreous and denser than W64Ao2 parent, and similar phenotypes were observed for pooled samples of vitreous and opaque kernels.

To identify chromosomal regions linked with endosperm modification, DNA in bulked samples of F2 vitreous and opaque individuals was analyzed with 140 polymorphic SSR primers distributed across the 10 maize chromosomes. Figure 1 shows the map location of the SSR markers used to analyze the K0326Y QPM by W64Ao2 cross. Although multiple SSRs were tested, we were unable to find polymorphic markers that mapped to bins 3.00, 3.10, 4.00, 4.11, 5.06, 6.03, 8.00, 8.08, 9.06, 10.00, 10.01 and 10.05, many of which correspond to where telomeres occur. For the

CM105*Mo2* by W64A*o2* cross, the bulks were analyzed with 138 informative SSR markers (Supplemental Table 1), which covered most of the genome with the exception of bins 2.03, 2.10, 3.00, 3.10, 4.00, 4.11, 5.09, 8.0, and 8.09, most of which are also telomeric regions.

The BSA of the K0326Y QPM by W64Ao2 cross identified regions on chromosomes 7 and 9 that are linked with *Opm* loci (Table 3). Linked SSR markers on chromosome 7 were found near the centromeric region in bin 7.02 (umc1016, umc1929, umc1393, 27-kDa γ-zein, bnlg1022a), while those on chromosome 9 are in bins 9.03 (phi022, bnlg127, and bnlg1714) and 9.05 (umc1078). For the CM105*Mo2* by W64A*o2* cross, regions on chromosomes 7 and 6 were found to be linked with *Opm* loci (Table 4). Among the markers near the centromeric region of chromosome 7 (umc1016, umc1393, 27-kDa γ-zein, bnlg1022a) were several also identified in the K0326Y QPM by W64Ao2 cross. There were two regions on chromosome 6, one associated with bins 6.03/6.04 (umc1887 and umc1014) and a second one in bin 6.05 (mmc0241). Because recombination is more frequent the further away a marker is from an *Opm* locus, a polymorphic marker linked with an *Opm* locus should show significant differences in frequency between the two bulks, and the allele frequency within the bulks should be complementary and deviate from the expected ratio of 1:1 for an unlinked marker (Quarrie et al. 1999). To assess the validity of whether or not an *Opm* locus was present in each of these chromosomal regions, the DNA from each individual in a bulk was assayed with informative SSR markers and a χ^2 test performed. The results showed that the segregation for all the *Opm*-linked markers deviated significantly from a 1:1

Table 2 Phenotypic characterization of the CM105*Mo2* and W64A*o2* inbred lines, and the pooled vitreous and opaque F3 progeny from the CM105*Mo2* by W64A*o2* cross

Phenotype	CM105*Mo2*	W64A*o2*	Vitreous bulk	Opaque bulk
Vitreousness	178.5 ± 41.7 a	31.1 ± 12.6 b	211.7 ± 21.6 c	15.7 ± 8.2 d
Density (g/mL)	1.3 ± 0.02 a	1.1 ± 0.02 b	1.3 ± 0.04 a	1.1 ± 0.05 b

The value shown is the average and standard deviation for the given traits. Within a row, values with the same letter are not significantly different at $P = 0.05$, based on the LSD method
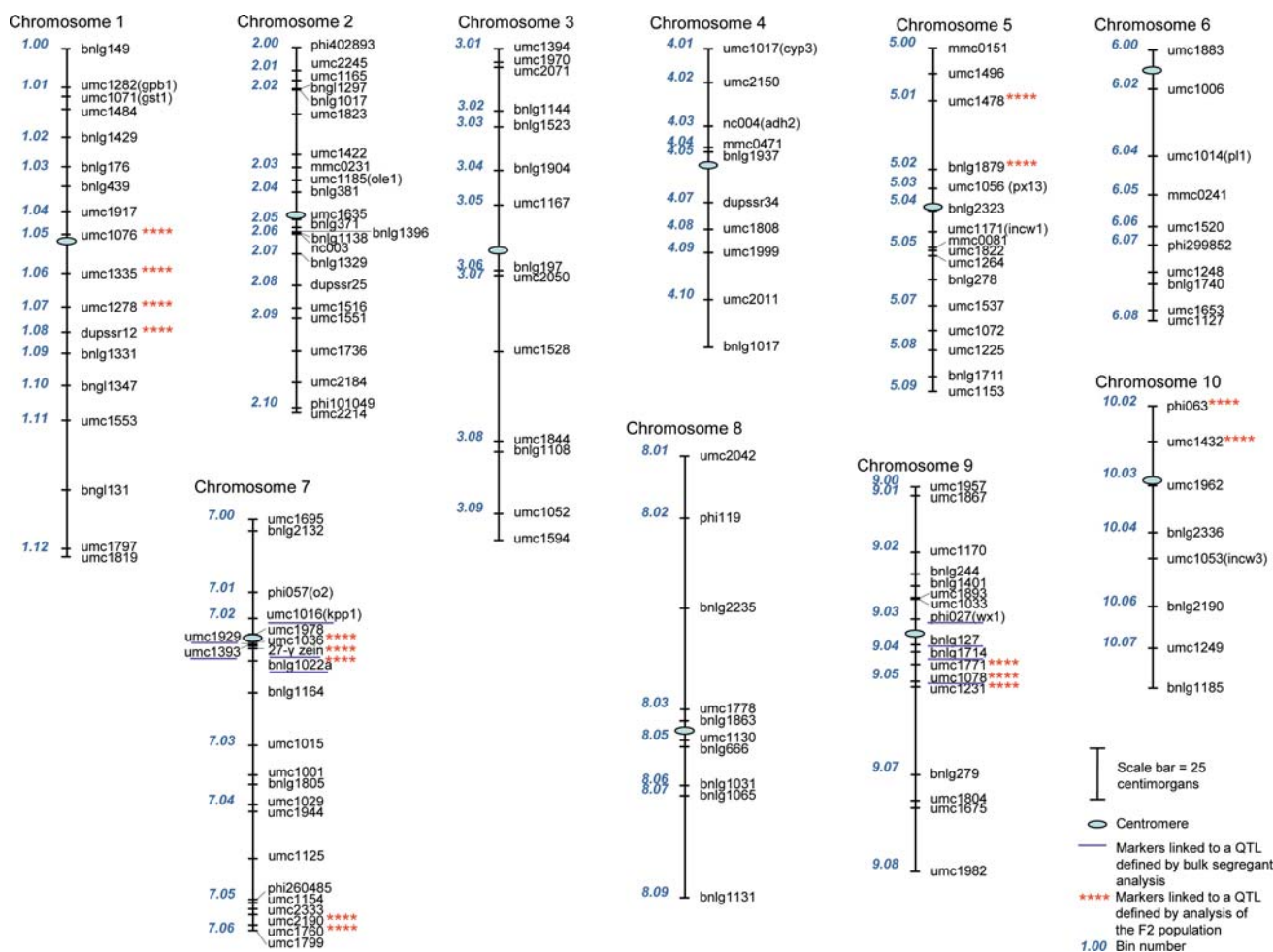
Fig. 1 A genetic linkage map constructed with polymorphic SSR markers used for analysis of the K0326Y QPM by W64A*o2* crosses

ratio, indicating that these chromosomal regions are likely to contain a locus associated with the *Opm* phenotype (Tables 3, 4).

QTL mapping with a K0326Y QPM by W64A*o2* F2 population

The BSA approach for identifying chromosomal regions associated with a trait is useful for F2 populations showing continuous phenotypic variation, like the vitreous kernel phenotype in QPM. However, it only allows the detection of major QTLs, and it is not possible to estimate their relative contribution to the trait. We found it was possible to make a quantitative measurement of the degree of vitreousness by using a digital camera to determine the light transmitted through a single kernel. For this analysis, kernels were removed from the middle of a well filled F2 ear of the K0326Y QPM by W64A*o2* cross, photographed, tested for hardness by the Instron assay, and then germinated on sterile culture medium for DNA isolation. Some embryos failed to germinate because they were damaged either by

the Instron procedure or excessive bleach penetration into the cracked kernel during seed surface sterilization. Of the initial 300 kernels, 229 germinated and yielded DNA for SSR marker analysis. A linkage map was developed based on 140 informative SSR markers (Fig. 1). The average spacing was 15.3 cM, but there were five gaps larger than 40 cM (one on chromosome 3 in bin 3.07, three on chromosome 8 in bins 8.02 and 8.08 and one on chromosome 9 in bin 9.06) and six gaps larger than 30 cM (one in bin 1.11, one each in bin 3.07 and 3.08, one in bin 7.00, one in bin 8.01 and one in bin 9.07). Chromosome 8 had the largest gaps and the largest average linkage distances with an average of 24.1 cM between markers.

Based on simple interval mapping using MapManager QTX (Manly et al. 2001), seven QTLs associated with the modified *o2* kernel phenotype were identified (Table 5). The two most significant QTLs are in bins 7.02 and 9.04/9.05, with LRS values of 75.3 and 29.4, respectively. Both of these QTLs had additive effects and were contributed by the K0362Y QPM parent. QTLs with somewhat smaller effects (LRS values between 13 and 17) were found in bins

Table 3 Segregation of SSR markers linked to an *Opm* locus in a cross of K0326Y QPM by W64A*o2*

Marker	Chromosome	Vitreous bulk					Opaque bulk				
		A	H	B	χ^2	P	A	H	B	χ^2	P
umc1016	7.02, S	34	4	0	59	***	3	2	35	49	***
umc1929	7.02, L	28	10	0	39	***	1	2	37	63	***
umc1393	7.02, L	36	3	0	64	***	1	1	38	66	***
27-kDa γ-zein	7.02, L	36	3	0	64	***	1	0	37	66	***
bnlg1022a	7.02, L	29	5	1	43	***	0	2	38	70	***
phi022	9.03, S	19	15	3	13	***	2	12	25	25	***
bnlg127	9.03, S	19	15	5	9	***	0	13	26	33	***
bnlg1714	9.04, S	21	14	4	14	***	1	13	26	30	***
umc1078	9.05, L	24	12	3	21	***	1	13	25	28	***

Chromosomal bin numbers and arm designations are listed for each marker. Chi-squared statistics and levels of statistical significance, *P*, are shown for each marker; *** indicates $P < 0.001$

A number of plants homozygous for the K0362Y QPM allele, *H* number of plants heterozygous for both parental alleles, *B* number of plants homozygous for the W64A*o2* allele

Table 4 Segregation of SSR markers linked to an *o2*-modifier locus in a cross of CM105*Mo2* by W64A*o2*

Marker	Chromosome	Vitreous bulk					Opaque bulk				
		A	H	B	χ^2	P	A	H	B	χ^2	P
umc1887	6.03, L	20	7	1	24	***	2	10	16	13	***
umc1014	6.04, L	24	4	0	41	***	2	7	19	19	***
mmc0241	6.05, L	24	1	0	44	***	4	9	15	7.8	***
umc1016	7.02, S	16	12	0	17	***	1	13	14	5.5	*
umc1393	7.02, S	18	9	1	19	***	2	15	11	5.2	*
27-kDa γ-zein	7.02, S	15	9	1	14	***	2	14	12	3.2	*
bnlg1022a	7.02, S	18	8	1	20	***	2	14	12	6.4	*

Chromosomal bin numbers and arm designations are listed for each marker. Chi-squared statistics and levels of statistical significance, *P*, are shown for each marker; *** indicates $P < 0.001$, * indicates $0.01 < P < 0.05$

A number of plants homozygous for the CM105*Mo2* allele, *H* number of plants heterozygous for both parental alleles, *B* number of plants homozygous for the W64A*o2* allele

1.05/1.06, 1.07/1.08, 5.01/5.02, 7.05 and 10.02. The K0326Y QPM parent was also the source of these QTLs, and with the exception of those in bins 5.01/5.02 and 7.05, which had dominant effects, they also had additive effects.

Expression profiling identifies a small group of candidate modifier genes, several of which map at or close to QTLs

As an initial approach to identify candidate genes corresponding to *Opm* QTLs, we analyzed RNA transcripts from true-breeding vitreous and opaque F4 kernels from the K0326Y QPM by W64A*o2* cross. For this experiment we selected 20 ears of each phenotypic class, and these were divided into 4 biological sample pools of 5 ears each (see "Materials and methods"). Following RNA extraction of the pooled kernels, Cy3- and Cy5-labeled cDNA targets were amplified by in vitro transcription and hybridized to the maize 46 K version 1 oligonucleotide array, which consists of 46,128 probes. Only 24 genes were found to have significantly increased expression in vitreous kernel pools, and interestingly no genes were found to have reduced expression in vitreous pools (Table 6). The sequences of the oligonucleotide probes were used to identify mapped EST contigs; these were then used for checking and, in some cases, revising the annotations for the 46 K array provided at http://www.maizearray.org. With this information it was possible to establish map positions for all of the differentially expressed genes (see "Materials and methods") and these are shown in Table 6.

To confirm the gene expression differences revealed by the microarray hybridization, real time quantitative PCR was used to re-examine the transcript levels of most of the differentially expressed genes. Genes with small fold-change differences in expression and a sequence annotation that did not suggest a putative function were not re-tested. The fold-change values of the genes for which differential expression was confirmed are shown in Table 6, including a number of genes which map very close to the QTLs.

Table 5 Chromosome map position and effect of significant QTLs involved in *o2* modification, as measured by vitreousness and hardness

Bin	Trait	Flanking SSR marker	LRS	PEV	Additive effect	Dominant effect
1.05–1.06	Vitreous	umc-1076–umc-1335	12.8	5	−13.43	11.01
1.07–1.08	Vitreous	umc1278–dupss12	13.8	6	−15.63	−1.52
5.01–5.02	Vitreous	umc1478–bnlg1879	14.1	6	0.01	−27.8
7.02	Vitreous	umc1978–bnlg1022	75.3	28	−32.96	−0.06
7.05	Vitreous	umc2190–umc1760	14.1	6	10.02	−18.70
9.04-9.05	Vitreous	umc1771–umc1231	29.4	12	−18.90	−9.36
10.02	Vitreous	phi063–umc1432	16.7	11	−16.60	−9.19

The QTLs were identified by composite interval mapping of a segregating F2 mapping population. LRS is the likelihood ratio statistic that measures the significance of the QTL. PEV (percent explained variance) is the percent of total variance explained by the QTL. The value of the additive and dominant effects is negative if the presence of a K0326Y QPM allele tends to increase the vitreous trait

Table 6 Genes identified as differentially expressed between vitreous and opaque kernels derived from the K0326Y QPM by W64A*o2* cross

Putative Gene Identity	Array ID	mRNA accession #	Bin	Coordinate	Fold increase in vitreous pools (microarray)	Fold increase in vitreous pools (real time PCR)
NADH: ubiquinone oxidoreductase subunit 4	MZ00036508	AY104931	1.05	439.1	1.5	−1.4 (± 0.2)[a]
Probable small nucleolar RNA associated protein 1[a]	MZ00014004	DQ245612	5.03	232.03	3.3	NA[a,b]
Endomembrane protein 70-like protein	MZ00027277	BT024118	6.06	435.05	1.9	2.1 (± 0.6)
Glucose transporter	MZ00029899	AY106711	7.02	253.05	1.9	1.5 (± 0.2)
27-kDa γ-zein[c]	NA[c]	AY109329	7.02[c]	258.4	–	4.1 (± 0.1)
Ethylene-responsive element binding protein[c]	NA[c]	AY105702	7.02[c]	258.4	–	2.6 (± 0.3)
Alanine aminotransferase[c]	NA[c]	AY105956	7.02[c]	258.4	–	−2.6 (± 0.7)
26S proteasome regulatory subunit-like protein[d]	MZ00025689	DQ245134	7.02[d]	254.05	3.5	14.9 (± 1.2)
26S proteasome regulatory particle non-ATPase subunit3[d]	MZ00024036	AY103743	7.02[d]	193.00	4.1	−1.3 (± 0.2)[a]
Putative protein phosphatase type 2C	MZ00016817	BT02415	7.03	384.03	2.0	56.4 (± 5.6)
Weakly similar to soybean sorbitol-like transporter	MZ00020679	AY111942	7.04	431.1	1.8	4.5 (± 1.0)
Plenty-of-prolines-101	MZ00056560	DR828623	7.05	548.17	1.4	1.4 (± 0.2)
Pyrophosphate–fructose 6-phosphate 1-phosphotransferase α subunit	MZ00015645	BT017003	9.03	226.04	5.2	16.0 (± 1.7)
Zinc finger protein	MZ00038867	CD966007	9.03	254.03	1.9	1.7 (± 0.1)
A, β-fold hydrolase 1	MZ00025901	AY105548	9.04	317.04	2.5	4.9 (± 0.2)
EIN3-like protein	MZ00042403	CFO56286	9.05	342.04	3.3	1.4 (± 0.1)

[a] Although the microarray and real-time PCR gave discrepant results, data are presented for these genes because they apparently map at or very close to QTLs

[b] Two PCR products were amplified in all opaque pools, whereas a single product was amplified in all vitreous pools, and it was therefore not possible to obtain an expression ratio

[c] The 27-kDa γ-zein gene and the ethylene-responsive element binding protein gene are in the same BAC contig (#314) and were identified as differentially expressed by real-time PCR

[d] These genes have different map coordinates and no sequence homology

Among these are several genes in bin 7.02, and it is possible that more than one of them contributes to the major QTL in this region. An ethylene-insensitive 3 (*EIN3*)-like gene coincides with a QTL in bin 9.05.

Table 6 also includes several genes for which the real-time PCR results did not confirm the microarray result. These data are presented because the genes apparently map at or very close to QTLs; we are investigating their possible differential expression using parental allele-specific qRT-PCR analysis. Among these are genes with similarity to NADH: ubiquinone oxidoreductase subunit 4, which occurs in chromosome bin 1.05, a small nucleolar RNA-associated protein in bin 5.03, and a 26S proteasome regulatory protein in bin 7.02 (MZ00024036).

Given the increase in 27-kDa γ-zein protein in QPM (Geetha et al. 1991; Lopes and Larkins 1991) and that an *Opm* QTL in bin 7.02 maps near the 27-kDa γ-zein locus, we were somewhat surprised that this gene was not among those identified as differentially expressed in the microarray output. When the hybridization intensity values of the microarray probes were examined, the results showed that this gene is very highly expressed, as would be expected for a major storage protein. We set the laser scanning intensity to detect expression for the maximal number genes, and at this setting, highly expressed genes, such as those encoding zein storage proteins, might have been saturated. Despite this, we could often detect increased expression of the 27-kD γ-zein gene in the vitreous pools (data not shown). However, between arrays the results were variable, and as a consequence the 27-kDa γ-zein was excluded due to the stringency of the statistical analysis. We therefore included this gene in the real-time PCR analysis. We also tested the expression of 12 other predicted genes that occur in BAC contig #314 of the maize FPC map (http://www.genome.arizona.edu/fpc/maize/), which contains the 27-kDa γ-zein gene, since any of these genes could theoretically account for a QTL at this location. The BAC containing the 27-kDa γ-zein gene (ZMbb049I19; Accession #AC217110) also contains the 50-kDa γ-zein, a putative alanine aminotransferase gene and two other genes (Fig. 2). The results showed that two genes in contig 314, the 27-kDa γ-zein and a gene encoding an ethylene-responsive element binding-protein (EREBP) homologue, were more highly expressed in the vitreous than the opaque endosperm pools (Table 6).
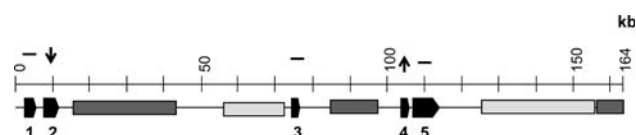
Fig. 2 Physical map of BAC clone ZMbb049I19. The BAC occurs in contig 314 with genetic marker umc1393 (258.4 cM) and the following physical markers: CL2764, CL1979, PCO123780, PCO137477 and zp27. The flanking genetic markers are umc1929 (249.1 cM) in contig 310 and bnlg1022a (274 cM) in contig 316. The orientation of the predicted genes is indicated with *solid black arrows* and they are numbered as follows: *1*, putative 5′-phosphoribosyl-5-aminoimidazole synthetase; *2*, putative alanine aminotransferase; *3*, 50-kDa γ-zein; *4*, 27-kDa γ-zein; *5*, hypothetical protein (fiber protein-like). The *upward pointing arrows* indicate increased expression; *downward arrows* indicate reduced expression and *horizontal lines* indicate no change in expression. *Dark shaded boxes* show Ty3/*gypsy* retrotransposons, and *light shaded boxes* show Ty1/*copia* retrotransposons

Although the EREBP gene does not occur in BAC ZMMBBb0049I19 (Fig. 2), it occurs in a different BAC (ZMMBBc0273I06; Accession #AC197252-3) that includes the 27-kDa γ-zein gene where they are separated by approximately 104 kb. The gene encoding the 50-kDa γ-zein in BAC ZMMBBb0049I19 and eight other predicted genes in contig 314 showed no difference in expression between the vitreous and opaque phenotypic classes (data not shown). The alanine aminotransferase gene in BAC ZMMBBb0049I19 is down-regulated in the vitreous pools (Table 6), further demonstrating that increased transcription is not a general feature of the genes in this region.

Discussion

The nature and relationships between *Opm* genes in most QPM germplasms is unknown. Early studies suggested there were likely to be multiple un-linked *Opm* loci with positive and negative effects. Belousov (1987) reported that many of these genotypes have a complex system of genetic control, with dosage effects, cytoplasmic effects, and incomplete and unstable penetrance of the *Opm* genes. Additive, dominant, semi-dominant and recessive gene action was postulated for different genetic backgrounds. We reported the phenotypic and genotypic analysis of *Opm* loci in CIMMYT's Pool 33 based on the BSA approach and a limited set of RFLP markers (Lopes and Larkins 1995; Lopes et al. 1995). The phenotypic analysis suggested two independent loci affecting seed density and opacity, and two QTLs affecting these traits were found, one near the centromere of chromosome 7 that is linked with the 27-kDa γ-zein gene, and a second locus near the telomere of the long arm of chromosome 7. The nature of this analysis did not allow us to assess the relative contribution of each of these loci to the modified *o2* phenotype.

The initial goal of this study was to investigate the relationships between *Opm* loci in CM105*Mo2* (Pool 33 QPM) and a South African QPM, K0326Y. We used W64A*o2* as the common soft *o2* parent for these experiments, because it differs markedly from the QPM inbreds in vitreousness, density and hardness (Tables 1, 2), and we hoped to be able to determine if there were common genetic determinants influencing each of these traits. Seed density and vitreousness appear to be correlated (Lopes and Larkins 1995), but it is technically easier to measure density. We found that the simplest method to measure vitreousness was to place kernels on a light box and photograph them with a digital camera, and then measure light transmission in arbitrary units using Adobe Photoshop. We later became aware of a study by Erasmus and Taylor (2004) that described a very similar method for measuring vitreousness.

Using the BSA approach to compare the K0326Y QPM and CM105*Mo2* by W64A*o2* crosses, we were able to identify three *Opm* QTLs in each genetic background: the K0326Y QPM by W64A*o2* cross revealed QTLs in bins 7.02, 9.03 and 9.05, while the CM105*Mo2* by W64A*o2* cross identified QTLs in bins 7.02, 6.03/6.04 and 6.05. The QTL in bin 7.02 appears to be common to both genetic backgrounds, as it was identified with many of the same SSR markers (Tables 3, 4); it is likely that this locus corresponds to the QTL identified by Lopes et al. (1995).

We extended the analysis of the K0326Y QPM by W64A*o2* cross by analyzing single kernels of an F2 ear. In addition to measuring light transmission (vitreousness) with a digital camera, we also made Instron measurements to determine kernel hardness. The results showed a 50-fold range in light transmission, with the vitreous kernels tending to be harder than the opaque kernels. There was a low correlation ($R^2 = 0.11$) between vitreousness and hardness, but it is possible that the hardness data are unreliable, since only a single kernel breakage measurement could be made. We are developing recombinant inbred lines from the progeny of this cross, and they will allow us to collect hardness data for a larger number of kernels with a uniform genotype.

Based on segregation of vitreousness in the F2 population, seven *Opm* QTLs were identified that accounted for approximately 75% of the phenotypic variation. The loci in bins 7.02 and 9.04/9.05, which correspond to the QTLs identified in the BSA, had LRS values of 75.3 and 29.4, respectively, and thus are strong candidates for QTLs. These two QTLs accounted for 40% of the phenotypic variation. The QTLs in bins 1.05/1.06, 1.07/1.08, 5.01/5.02 and 10.02 have smaller LRS values and therefore might be discounted. However, other evidence suggests their validity (see below). There are gaps in some of the chromosome linkage maps due to a limited number of markers in certain regions. Thus, the QTLs that account for the remaining

25% of variation in the vitreous phenotype could have been missed.

In the analysis of Pool 33 QPM, Lopes et al. (1995) reported a QTL near the telomere of the long arm of chromosome 7 that was identified by a single RFLP marker, umc35. This locus was detected in the BSA of a Pool 33 by W22*o2* cross, but not the Pool 33 by W64A*o2* cross. The umc35 marker is in bin 7.05, and the size of the effect of this QTL, as measured in the F2 population derived from the cross between K0326Y QPM and W64A*o2* (Table 5), could explain why it might not have been detected by BSA. The microarry analysis (see below) identified candidate genes that map to bins 1.05/1.06 and 9.04/9.05, which supports the validity of these QTLs.

The mechanism by which *Opm* genes create a vitreous kernel phenotype is not understood. Although they could be related, it is possible that the genes responsible for *o2* modification are different from those that cause the wild type vitreous phenotype (Séne et al. 2001). To a large extent the mechanisms that cause a starchy endosperm in opaque mutants are not well characterized (Hunter et al. 2002). The *O2* gene encodes a transcription factor that regulates a number of genes expressed in the endosperm, including those encoding 22-kDa α-zein proteins (Schmidt 1993). The reduced size of zein protein bodies in *o2* mutants was thought to explain the opaque kernel phenotype (Geetha et al. 1991), although this was a tenuous hypothesis, because the *o2* mutation influences expression of many genes (Hunter et al. 2002; Gibbon et al., unpublished data). However, it was shown that silencing the genes encoding 22-kDa α-zeins by RNAi was sufficient to create an opaque kernel phenotype (Segal et al. 2003). The abnormal localization of 22-kDa α-zeins in *floury1* appears to be responsible for the starchy endosperm of this mutant (Holding et al. 2007). Thus, the reduced synthesis or altered deposition of 22-kDa α-zeins could be responsible for a starchy endosperm phenotype.

Other mutations that alter zein synthesis or disrupt protein body structure are associated with an opaque endosperm phenotype. For example, the *floury2* (*fl2*) and *Defective endosperm B30* (*De-B30*) mutations, which cause defective signal peptides in α-zeins (Coleman et al. 1997; Kim et al. 2004), disrupt the organization of zeins in the protein body and cause an elevated unfolded protein response (UPR) (Kaufman 1999). Reduced levels of the 27-kDa γ-zein in the *o15* mutant (Dannenhoffer et al. 1995) and a deletion mutation in the 16-kDa γ-zein in the *Mucuronate* (*Mc*) mutant (Kim et al. 2006) are also associated with the UPR and a starchy endosperm phenotype. These observations are consistent with the hypothesis that the size, number and structure of protein bodies influence the texture and vitreous phenotype of the mature endosperm (Kim et al. 2004, 2006).

Biochemical characterization of QPM showed a distinctive difference in zein composition relative to soft *o2* mutants. Although QPMs have reduced levels of 22-kDa α-zeins, typical of *o2* mutants, they contain approximately twice as much 27-kDa γ-zein as starchy *o2* genotypes (Ortega and Bates 1983; Wallace et al. 1990). Two studies demonstrated a positive relationship between the content of 27-kDa γ-zein and *Opm* gene dosage (Geetha et al. 1991; Lopes and Larkins 1995). The 27-kDa γ-zein appears to initiate the formation of protein bodies (Lending and Larkins 1989; Coleman et al. 1996), and endosperms with increased amounts of this protein contain more protein bodies (Dannenhoffer et al. 1995). Because the 27-kDa γ-zein becomes cross-linked by disulfide bonds during kernel desiccation (Lopes and Larkins 1991), it was hypothesized that it, along with other cysteine-rich proteins, contributes to the formation of a covalently linked proteinaceous network around the starch grains (Dannenhoffer et al. 1995). Thus, the level of 27-kDa γ-zein could be an important component of endosperm modification in QPM, and the increased transcription of genes encoding this protein (Table 6) is consistent with this hypothesis.

A QTL identified by BSA mapped to bin 9.03, which includes the *waxy1* (*wx1*) locus as well as several other genes involved in starch biosynthesis. We previously reported a link between starch structure and vitreousness in QPM (Gibbon et al. 2003), and there is other evidence supporting such a relationship. *wx1* is a mutation of the gene encoding granule-bound starch synthase (GBSS I), and starch grains in homozygous mutants contain amylopectin but not amylose (Nelson and Rines 1962). How this compositional change affects the molecular structure of the starch grain is poorly understood, but when placed on a light box the mutant kernels are opaque. Many starch mutants have a reduced zein content (Tsai et al. 1978; Giroux et al. 1994), which complicates interpretation of their phenotypes based solely on changes in starch synthesis.

To identify potential candidate genes for the *Opm* QTLs in our mapping populations, we conducted a microarray experiment in which we made use of the individuals composing the true-breeding vitreous and opaque bulks made from the K0326Y QPM by W64A*o2* cross. The design of this experiment provided effective selection for genes associated with *o2* endosperm modification that are differentially expressed in what will become vitreous versus opaque endosperm at kernel maturity. Endosperm from 18-DAP kernels was chosen for this analysis, because it represents a mid-development stage with the highest levels of mRNA transcripts.

Surprisingly, a relatively small number of differentially expressed genes were identified with an oligonucleotide array of 46,128 probes. This may reflect the effectiveness of the pooling in our experimental design, but it is likely that there were many minor changes in transcript levels that

could not be detected by this analysis. The 27-kDa γ-zein is a good example. This gene is highly expressed in modified and starchy *o2* endosperm but was not identified as differentially expressed in the microarray analysis, probably as a result of signal saturation at the chosen laser scanning level. It is possible that additional and perhaps more extensive changes in gene expression would be detected by examining later stages of development; however, following 18-DAP the endosperm contains an increasing proportion of cells undergoing programmed cell death (PCD) (Woo et al. 2001) and this would create another factor affecting the results. The fact that genes with both abundant and rare transcript levels were detected by this analysis, and that there is a physiological connection between many of them, supports the validity of the microarray results.

Several of the differentially expressed genes map coincidentally with the *Opm* QTLs in bins 1.05, 7.02 and 9.05 (Tables 5, 6). The QTL in bin 7.02 occurs near the 27-kDa γ-zein locus, similar to our previous results (Lopes et al. 1995). The level of the 27-kDa γ-zein protein is consistently increased in modified *o2* kernels (Lopes and Larkins 1995), but whether the higher amount of 27-kDa γ-zein is the cause or an effect of *Opm* gene activity remains to be established. When a QTL is coincident with a modifier gene, there should be an identifiable sequence difference associated with the gene or its regulatory region between the *o2* and modified *o2* backgrounds. Such a mutation would be defined as *cis*-acting and because it could be within the transcribed sequence or its regulatory regions, it could be hundreds of kb away and very difficult to define. Differentially expressed genes that do not map to QTLs may be under the direct control of *trans*-acting modifying factors, or their altered expression may simply be indirect, reflecting downstream effects of changes in kernel composition or modifier gene expression.

In an attempt to identify genetic changes in the 27-kDa γ-zein gene that might help to explain its role in modification, we sequenced its coding and 5′-flanking regions and made comparisons between W64A+, W64A*o2* and several different QPM lines. We found no consistent sequence differences that could potentially account for a QTL (data not shown), although we cannot rule out the possibility that one or more QTLs reside in a distant regulatory sequence. It is also possible that the differential expression of the 27-kDa γ-zein gene results from trans-acting factors, which could be QTLs. To establish whether the expression of modifier genes is affected by *cis*-acting mutations or by *trans*-acting factors, we will need to perform allele specific expression analysis between the modified *o2* and *o2* parental lines and determine the ratios of the parental transcripts in reciprocal F1 s (Hochholdinger and Hoecker 2007).

A number of the differentially expressed genes identified in the microarray experiment have been implicated in PCD. PCD is a normal part of maize endosperm development; it begins in the center during early development and eventually spreads as far as the aleurone cells. Ethylene signaling was shown to be involved in endosperm PCD (Young et al. 1997), and it is interesting that two genes involved in ethylene signaling (an *EIN3*-like gene and an ethylene-responsive element binding-protein, EREBP) are up-regulated in modified *o2*. In Arabidopsis, EIN3 serves as a primary transcription factor that plays a central role in ethylene signaling by activating secondary transcription factors, including EREBPs, which activate the ultimate effectors of the ethylene response (Guo and Ecker 2004). Both of these components of ethylene signaling were found to be up-regulated in recent transcript profiling experiments focusing on PCD in barley endosperm (Sreenivasulu et al. 2006). The type 2c protein phosphatase has similarity to ABI1 and ABI2 proteins, which are negative regulators of ABA signaling (Hirayama and Shinozaki 2007), and it is strongly up-regulated in modified *o2*. Interestingly, ABA has been shown to have an inverse effect to ethylene, since it represses PCD in the endosperm (Young and Gallie 2000). Glucose is known to play an antagonistic role to ethylene in that it promotes the degradation of the EIN3 protein (Yanagisawa et al. 2003). Several genes encoding proteins that may play a role in glucose homeostasis are also up-regulated. These include pyrophosphate-fructose 6-phosphate 1-phosphotransferase, which, along with ATP-dependent phosphofructokinase, catalyzes the first committed step of glycolysis. The α-subunit of the 26S proteasome was found to be strongly up-regulated in modified *o2*, and there is evidence that the 26S proteasome complex is involved in the protein turnover that occurs during PCD (Smalle and Vierstra 2004). Exactly how increasing PCD might promote the formation of vitreous endosperm in modified *o2* is unclear, but studies aimed at investigating this possibility are underway. As several of the candidate genes may be linked to ethylene and ABA signaling, which could affect a variety of cellular processes, it is possible that other pathways associated with these hormones play a role in *o2* endosperm modification.

References

Belousov AA (1987) Genetic analysis of modified endosperm texture in *opaque2* maize. Sov Genet 23:459–464

Bhan MK, Bhandari N, Bahl R (2003) Management of the severely malnourished child: perspective from developing countries. Br Med J 326:146–151

Bjarnason M, Vasal SK (1992) Breeding quality protein maize (QPM). Plant Breed 9:181–216

Coleman CE, Herman EM, Takasaki K, Larkins BA (1996) The maize γ-zein sequesters α-zein and stabilizes its accumulation in protein bodies of transgenic tobacco endosperm. Plant Cell 12:2335–2345

Coleman CE, Clore AM, Ranch JP, Higgins R, Lopes MA, Larkins BA. (1997) Expression of a mutant α-zein creates the *floury*2 phenotype in transgenic maize. Proc Natl Acad Sci USA 94:7094–7097

Dannenhoffer JM, Bostwick DE, Or E, Larkins BA (1995) *opaque*15, a novel mutation with properties of an *opaque*2 modifier. Proc Natl Acad Sci USA 92:1931–1935

Deutscher D (1978) The current status of breeding for protein quality in corn. In: Friedman M (ed) Nutritional improvement of food and feed grains. Plenum, New York, pp 281–300

Erasmus C, Taylor JRN (2004) Optimising the determination of maize endosperm vitreousness by a rapid non-destructive image analysis technique. J Sci Agric 84:920–930

Ewing B, Green P (1998) Base-calling of automated sequencer traces using phred II. Error probabilities. Genome Res 8:186–194

Ewing B, Hillier L, Wendl MC, Green P (1998) Base-calling of automated sequencer traces using phred I. Accuracy assessment. Genome Res 8:175–185

Geetha KB, Lending CR, Lopes MA, Wallace JC, Larkins BA (1991) *opaque*–2 modifiers increase gamma-zein synthesis and alter its distribution in maize endosperm. Plant Cell 3:1207–1219

Geevers HO, Lake JK (1992) Development of modified *opaque-2* maize in South Africa. In: Mertz ET (ed) Quality protein maize. American Association of Cereal Chemists, St. Paul, MN, pp 49–78

Gibbon BC, Wang X, Larkins BA (2003) Altered starch structure is associated with endosperm modification in quality protein maize. Proc Nat Acad Sci USA 100:15329–15334

Giroux MJ, Boyer C, Feix G, Hannah LC (1994) Coordinated transcriptional regulation of storage product genes in maize endosperm. Plant Physiol 106:713–722

Gordon D, Abajian C, Green P (1998) Consed: a graphical tool for sequence finishing. Genome Res 8:195–202

Guo H, Ecker JR (2004) The ethylene signaling pathway: new insights. Curr Opin Plant Biol 7:40–49

Habben JE, Larkins BA (1995) Improving protein quality in seeds. In: Kijel J, Galili G (eds) Seed development and germination. Marcel Dekker, NY, pp 791–810

Hirayama T, Shinozaki K (2007) Perception and transduction of abscisic acid signals: keys to the function of the versatile plant hormone, ABA. Trends Plant Sci 12:343–351

Hochholdinger F, Hoecker N (2007) Towards the molecular basis for heterosis. Trends Plant Sci 12:427–432

Holding DR, Larkins BA (2006) The development and importance of zein protein bodies in maize endosperm. Maydica 51:243–254

Holding DR, Otegui M, Li B, Meeley RB, Dam T, Hunter BG, Jung R, Larkins BA (2007) The maize *Floury1* gene encodes a novel ER protein involved in zein protein-body formation. Plant Cell 19:2569–2582

Hunter BG, Beatty MK, Singletary GW, Hamaker BR, Dilkes BP, Larkins BA, Jung R (2002) Maize opaque endosperm mutations create extensive changes in patterns of gene expression. Plant Cell 14:2591–2612

Kaufman RJ (1999) Stress signaling from the lumen of the endoplasmic reticulum: coordination of gene transcriptional and translational controls. Genes Dev 13:1211–1233

Kim CS, Hunter BG, Kraft J, Boston RS, Yans S, Jung R, Larkins BA (2004) A defective signal peptide in a 19-kD α-zein protein causes the unfolded protein response and an opaque endosperm phenotype in the maize *De*-B30* mutant. Plant Physiol 134:380–387

Kim CS, Gibbon BC, Gillikin JW, Larkins BA, Boston RS, Jung R (2006) The maize Mucronate mutation is a deletion in the 16-kDa γ-zein gene that induces the unfolded protein response. Plant J 48:440–451

Kniep KR, Mason SC (1989) Kernel breakage and density of normal and opaque2 maize grain as influenced by irrigation and nitrogen. Crop Sci 29:158–163

Lawrence CJ, Schaeffer ML, Seigfried TE, Campbell DA, Harper LC (2007) MaizeGDB's new data types, resources and activities. Nucleic Acids Res 35:D895–900

Li PX, Hardacre AK, Campanella OH, Kirkpatrick KJ (1996) Determination of endosperm characteristics of 38 corn hybrids using the Stenvert hardness test. Cereal Chem 73:466–471

Lending CR, Larkins BA (1989) A model for protein body formation in corn: immunolocalization of zeins in developing maize endosperm by light and electron microscopy. Plant Cell 1:1011–1023

Lopes MA, Larkins BA (1991) Gamma-zein content is related to endosperm modification in quality protein maize. Crop Sci 31:1655–1662

Lopes MA, Larkins BA (1995) Genetic analysis of *opaque2* modifier gene activity in maize endosperm. Theor Appl Genet 19:274–281

Lopes MA, Takasaki K, Bostwick DE, Helentjaris T, Larkins BA (1995) Identification of two *opaque2* modifier loci in quality-protein-maize. Mol Gen Genet 247:603–613

Manly KF, Cudmore RH Jr, Meer JM (2001) Map Manager QTX, cross-platform software for genetic mapping. Mamm Genome 12:930–932

Mertz ET (1992) Quality protein maize. American Association of Cereal Chemists, St. Paul, MN

Michelmore RW, Paran I, Keseli RV (1991) Identification of markers linked to disease-resistant genes by bulked segregant analysis: a rapid method to detect markers in specific genomic regions by using segregation populations. Proc Natl Acad Sci USA 88:9828–9832

Munck L (1992) The case of high-lysine barley breeding. In: Shewry P (ed) Barley, genetics, biochemistry, molecular biology and biotechnology. CAB International, Wallingford, pp 573–601

Nelson OE Jr, Rines HW (1962) The enzymatic deficiency in the waxy mutant of maize. Biochem Biophys Res Comm 9:297–300

Ortega EI, Bates LS (1983) Biochemical and agronomic studies of two modified hard-endosperm *opaque2* maize (*Zea mays* L.) populations. Cereal Chem 60:107–111

Pingali PL (2001) CIMMYT 1999–2000 Facts and trends meeting world maize needs. Technological opportunities and priorities for the public sector. CIMMYT, Mexico City

Prasanna BM, Vasal SK, Kassahun B, Singh NN (2001) Quality protein maize. Curr Sci 81:1308–1319

Quarrie SA, Lazic-Jancic V, Kovacevic D, Steed A, Pekic S (1999) Bulk segregant analysis with molecular markers and its use for improving drought resistance in maize. J Exp Bot 50:1299–1306

Schmidt RJ (1993) *Opaque2* and zein gene expression. In: Verma DPS (ed) Control of plant gene expression. CRC Press, Boca Raton, FL, pp 337–355

Segal G, Song R, Messing J (2003) A new opaque variant of maize by a single dominant RNAi-inducing transgene. Genetics 165:387–397

Séne M, Thévenot C, Hoffmann D, Bénétrix F, Causse M, Prioul J-L (2001) QTLs for grain dry milling properties, composition and vitreousness in maize recombinant inbred lines. Theor Appl Genet 102:591–599

Shen B, Carneiro N, Torresjerez I, Stevenson B, McCreery T, Helentjaris T, Baysdorfer C, Almira E, Ferl RJ, Habben JE, Larkins B (1994) Partial sequencing and mapping of clones from two maize cDNA libraries. Plant Mol Biol 26:1085–1101

Smalle J, Vierstra RD (2004) The ubiquitin 26S proteasome proteolytic pathway. Annu Rev Plant Biol 55:555–590

Sreenivasulu N, Radchuk V, Strickert M, Miersch O, Weschke W, Wobus U (2006) Gene expression patterns reveal tissue-specific signaling networks controlling programmed cell death and ABA-regulated maturation in developing barley seeds. Plant J 47:310–327

Tomkins JP, Davis G, Main D, Yim YS, Duru N, Muskat T, Goicoechea JL, Frisch DA, Coe EH Jr, Wing RA (2002) Construction and characterization of a deep-coverage bacterial artificial chromosome library for maize. Crop Sci 42:928–933

Tsai CY, Larkins BA, Glover DV (1978) Interaction of the *opaque-2* gene with starch-forming mutant genes on the synthesis of zein in maize endosperm. Biochem Genet 16:883–896

Vasal SK, Villegas E, Bjarnason M, Gelaw B, Goertz P (1980) Genetic modifiers and breeding strategies in developing hard endosperm *opaque2* materials. In: Pollmer WG, Phillips RH (eds) Quality traits of maize for grain and silage use. Martinus Nijhoff, London, pp 37–73

Vasil IK (1998) Biotechnology and food security for the 21st century: a real world perspective. Nat Biotech 16:399–400

Vieira J, Messing J (1982) The pUC plasmids, an M13mp7-derived system for insertion mutagenesis and sequencing with synthetic universal primers. Gene 19:259–268

Wallace JC, Lopes MA, Paiva E, Larkins BA (1990) New methods for extraction and quantification of zeins reveal a high content of gamma-zein in modified opaque-2 maize. Plant Physiol 92:191–196

Woo YM, Hu DWN, Larkins BA, Jung R (2001) Genomic analysis of genes expressed in maize endosperm identifies novel seed proteins and clarifies patterns of zein gene expression. Plant Cell 13:2297–2317

Yanagisawa S, Yoo SD, Sheen J (2003) Differential regulation of EIN3 stability by glucose and ethylene signaling in plants. Nature 425:521–525

Yim YS, Davis GL, Duru NA, Musket TA, Linton EW, Messing JW, McMullen MD, Soderlund CA, Polacco ML, Gardiner JM, Coe EH Jr (2002) Characterization of three maize bacterial artificial chromosome libraries toward anchoring of the physical map to the genetic map using high-density bacterial artificial chromosome filter hybridization. Plant Physiol 130:1686–1696

Young TE, Gallie DR (2000) Regulation of programmed cell death in maize endosperm by abscisic acid. Plant Mol Biol 42:397–414

Young TE, Gallie DR, DeMason DA (1997) Ethylene-mediated programmed cell death during maize endosperm development of wild type and *shrunken2* genotypes. Plant Physiol 115:737–751

Young VR, Scrimshaw NS, Pellet PL (1998) Significance of dietary protein source in human nutrition: animal and/or plant proteins? In: Waterlow JC, Armstrong DG, Fowden L, Riley R (eds) Feeding a world population of more than eight billion people. Oxford University Press in associate with Rank Prize Funds, New York, pp 205–221